

Relaxation of Spheromak Plasmas toward a Minimum-Energy State and Global Magnetic Fluctuations

A. Janos, G. W. Hart, and M. Yamada

Plasma Physics Laboratory, Princeton University, Princeton, New Jersey 08544

(Received 10 June 1985)

Globally coherent modes which are observed during formation in the S-1 Spheromak plasma occur during flux conversion and plasma relaxation toward a minimum-energy state, suggesting that these modes provide a means for relaxation. A significant finding is the temporal progression of these modes through a sequence $n = 5, 4, 3, 2$, $m = 1$, as q rises through rational fractions m/n , where n and m are defined by the functional dependence $e^{i(n\phi + m\theta)}$ of the fluctuations on toroidal angle ϕ and poloidal angle θ . Comparison with theory of the observed modes and the sequence of occurrence suggests that these modes are due to resistive MHD instabilities.

PACS numbers: 52.30.Jb, 52.55.Hc

A spheromak¹ is a toroidal magnetic-confinement configuration for plasmas. The toroidal field in the plasma is sustained entirely by poloidal plasma currents, eliminating the need to link the plasma topologically. An important observation in spheromak experiments^{2,3} is the tendency for plasmas to relax toward the force-free, minimum-energy Taylor⁴ state. In recent S-1 Spheromak experiments,^{5,6} magnetic flux conversion⁷ between the poloidal and toroidal fluxes of the plasma was observed during and after formation. This Letter presents the experimental identification and origin of magnetic fluctuations which occur during flux conversion and which, thus, may play a significant role in the relaxation process.

Flux conversion has become a topic of strong interest in the general plasma physics community since it has applications also to reversed-field pinches (RFP's) and tokamaks. This phenomenon is important not only for relaxation of these plasmas to a stable minimum-energy state, but also for sustainment.^{8,9}

Plasma formation in the S-1 Spheromak device is based on an inductive transfer of magnetic flux from a toroidal "flux core" to the plasma⁶ (Fig. 1). Currents from the toroidal- and poloidal-field capacitor banks induce poloidal and toroidal plasma currents simultaneously so that the magnetic configuration can be guided toward the Taylor state. Properly detailed programming of the formation process was found not to be essential since plasmas were observed^{5,6} to adjust themselves during formation to a final equilibrium near the Taylor state. The ratio of the toroidal plasma current to the toroidal magnetic flux in the plasma, I/Φ , assumed a constant value independent of initial conditions. In some cases, Φ was observed to exceed the toroidal flux in the core (by 40%, in some cases), giving clear evidence of conversion of poloidal to toroidal flux; this phenomenon could not be simulated with a two-dimensional formation and equilibrium code used earlier.¹⁰ I/Φ is proportional to the pinch parameter θ of RFP research through a simple

geometric factor involving the plasma size. It was observed experimentally in the S-1 device that this ratio I/Φ was maintained for the duration of a discharge. If the plasma evolved after formation such that the ratio I/Φ deviated too far from an acceptable range, then relaxation oscillations restored I/Φ to a range commensurate with that predicted on the basis of a force-free, minimum-energy state equilibrium. In an attempt to understand these phenomena further, a magnetic coil system external to the plasma was installed to look at magnetic fluctuations and their mode structure.

The S-1 device creates a plasma with a major radius of ~ 55 cm and a minor radius of ~ 30 cm. Toroidal plasma currents up to 350 kA are obtained. Peak plasma electron densities n_e range from 2×10^{13} to 1×10^{14} cm^{-3} for H_2 discharges; electron temperatures T_e range from 20 to 110 eV. The volume-average beta,

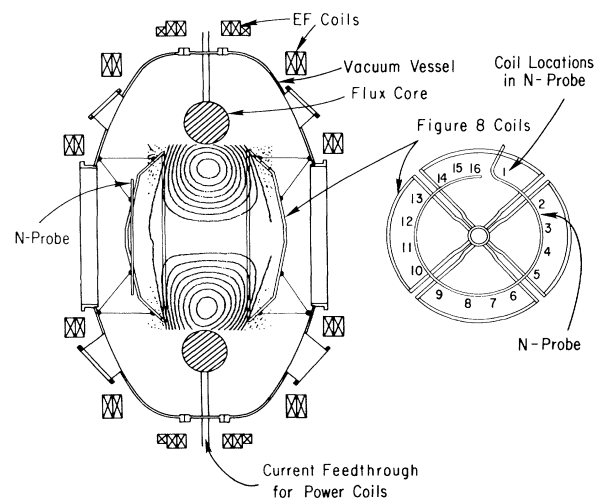


FIG. 1. Experimentally obtained Ψ contours of a spheromak configuration toward the end of the formation phase in the S-1 device.

β , is 5%–10%. Stability against rigid-body $n = 1$ modes is provided by passive figure-eight stabilization coils.⁶

The n -mode diagnostic coil array consists of sixteen pairs of coils distributed toroidally to measure major radius and toroidal components B_R and B_ϕ , respectively, inside the vacuum vessel at a major radius of 50 cm and an axial position of 60 cm (Fig. 1). The coils are located just outside the figure-eight coil system which is, in turn, outside the separatrix of the spheromak. Coils are designed to measure fluctuation levels of 1 G ($\sim 0.1\%$) in a typical frequency range of 5–10 kHz (bandwidth of 80 kHz). The B data are digitally integrated to obtain $B(\phi, t)$ which is then resolved into modes by use of discrete Fourier transformation.

The $q(\Psi)$ profile is obtained from $q(\Psi) = \Delta\Phi/\Delta\Psi$, where $\Delta\Phi$ is the difference in toroidal flux between two nearby poloidal flux surfaces Ψ and $\Psi + \Delta\Psi$, and Ψ and Φ are obtained from two-dimensional flux plots⁶ (Fig. 1).

Globally coherent fluctuations, hereafter called modes, are observed almost always during the formation phase (Fig. 2). The modes show a well-defined dependence $e^{i(n\phi + m\theta)}$ on toroidal angle ϕ and poloidal angle θ , with $1 \leq n \leq 5$, and $m = 1$. During formation, the magnetic configuration has a relatively large aspect ratio (≥ 2) so that the minor radius is well-defined and m is a good quantum number. B_R and B_ϕ data agree with respect to which modes are present and to their evolution, implying modes correspond to a helical deformation. Peak amplitudes relative to the unperturbed field are typically below 5%, while amplitudes as high as 20% were observed. After formation, the amplitudes are less than 1%.

The $n = 1$ mode is associated with a shift or tilt of the plasma and leads ultimately to the termination of

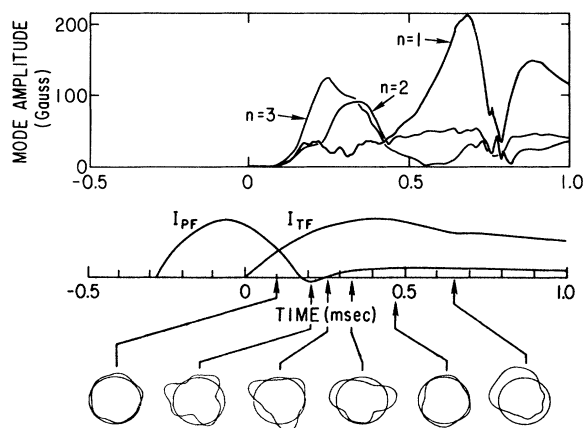


FIG. 2. Mode amplitude vs time showing a clear $n = 3, 2$ sequence. Formation is completed at 0.4 msec, and the discharge terminates at 0.75 msec. The toroidal dependence of B_R is shown with respect to the axisymmetric $n = 0$ component (circles). PF (TF) denotes poloidal (toroidal) flux.

the discharge for well-detached plasmas, while higher- n modes never cause termination. Modes always rotate in the electron diamagnetic drift direction ($\mathbf{B}_{\text{poloidal}} \times \nabla p$), the same as in tokamaks. Rotation velocities range from 0.12×10^6 to 1.2×10^6 cm/sec, $\sim \frac{1}{10}$ the Alfvén velocity. Occasionally, two modes are present simultaneously with velocities differing by as much as a factor of 3, suggesting that rotation is not associated with a rigid-body rotation. The rotation velocity often slows with time, indicating a possible dependence on B , n_e , or T_e . Fluctuation frequencies due to rotation range from 2 to 10 kHz and above.

Emissivity measurements, using a nineteen-channel array of silicon surface-barrier detectors sensitive to ultrasoft (≥ 10 eV) x-ray radiation, show a rotating $m = 1$ structure. Theory^{11,12} predicts that $m = 1$ modes are most unstable.

These modes are coincident in time with the plasma's relaxation to a Taylor state. The time evolution of poloidal and toroidal fluxes derived from flux plots shows a sudden (relative to the formation time) and sometimes large exchange of fluxes midway through the formation leading to a quiescent equilibrium, after formation, near the Taylor state. In Fig. 3, the poloidal flux [3(a)] captured by the spheromak drops precipitously during the same period that there is a large increase in the toroidal flux [3(b)] in the plasma. Figure 3(b) shows the toroidal flux within a closed poloidal flux surface defined by a constant poloidal-flux distance $|\Psi - \Psi_{\text{max}}| = 0.06$ V sec from Ψ_{max} , and includes over 50% of the total toroidal flux. The poloidal flux drops by $\sim 35\%$ (~ 0.06 V sec) as the toroidal flux increases by more than a factor of 6 (~ 0.025 V sec). Comparison of Φ curves for different $|\Psi - \Psi_{\text{max}}|$ reveals that toroidal flux is increased throughout the plasma and especially deep within the configuration. This behavior is interpreted as a relaxation since I/Φ adjusts toward that for a Taylor state and j/B ($= \lambda$) becomes nearly uniform over the plasma volume, where j is the current density. There is a sharp peaking of $n = 3$ and 2 mode activity between $t = 0.15$ and 0.25 msec, precisely when the fluxes are undergoing dramatic changes. After formation, the fluxes are observed to decay slowly because of resistive losses.

Experimental observations and comparison with theory suggest that the above modes are resonant inside the plasma and are resistive MHD unstable. A significant finding is the temporal progression of the MHD activity through an $n = 5, 4, 3, 2, m = 1$ mode sequence during formation (Fig. 2). Sequences are almost always from high n to lower n . The n th mode usually is decaying while the $(n - 1)$ th mode is growing. Higher- n -mode lobes are often observed to develop into lobes of the lower- n -mode structures. This progression is reminiscent of that for magnetic

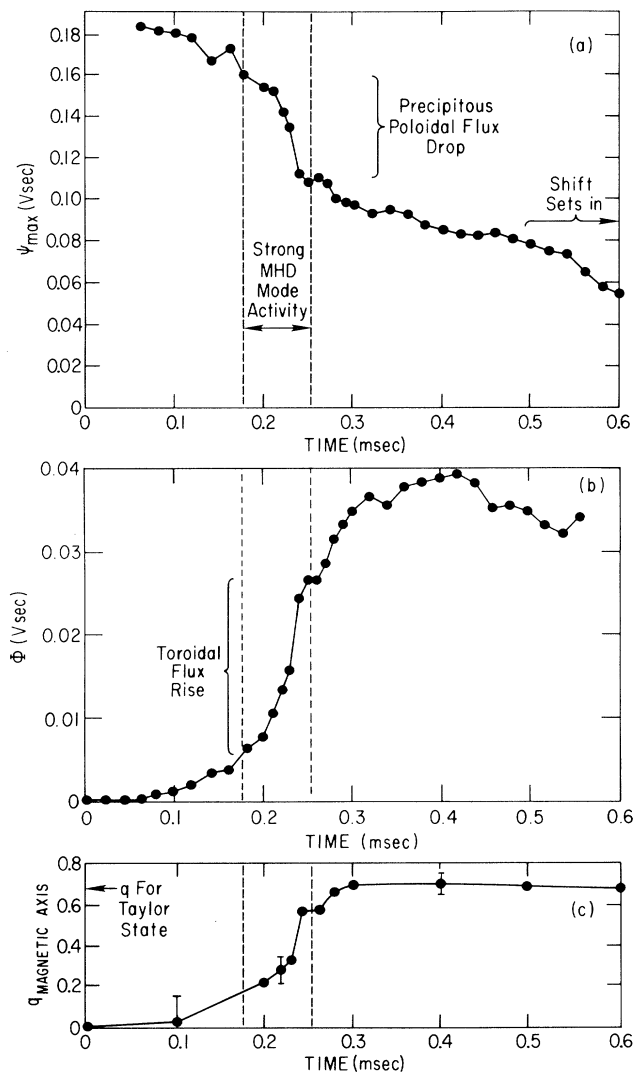


FIG. 3. Time evolution of (a) poloidal flux Ψ_{\max} , (b) toroidal flux Φ , and (c) q_0 . There is a precipitous drop in Ψ_{\max} and a concurrent sudden and large increase in Φ during mode activity.

oscillations during the startup phase of a tokamak plasma first observed¹³ in the early 1970's. In the tokamak case, a progression of $m = 6, 5, 4, 3, 2, n = 1$ modes is observed as $q(\Psi)$ decreases and $q = m/n$ rational surfaces enter the plasma; tearing modes are believed then to cause anomalous current penetration.¹⁴ A more recent theoretical study¹⁵ of the RFP startup phase has shown that anomalous current penetration can occur via a series of $m = 1$ globally reconnecting tearing modes that have sequential n numbers.

For the S-1 device, comparison of the time evolution of $q(\Psi)$ with that of the modes also shows a close relationship. The q value at the magnetic axis, q_0 , is observed to rise through the rational fractions $\frac{1}{5}, \frac{1}{4},$

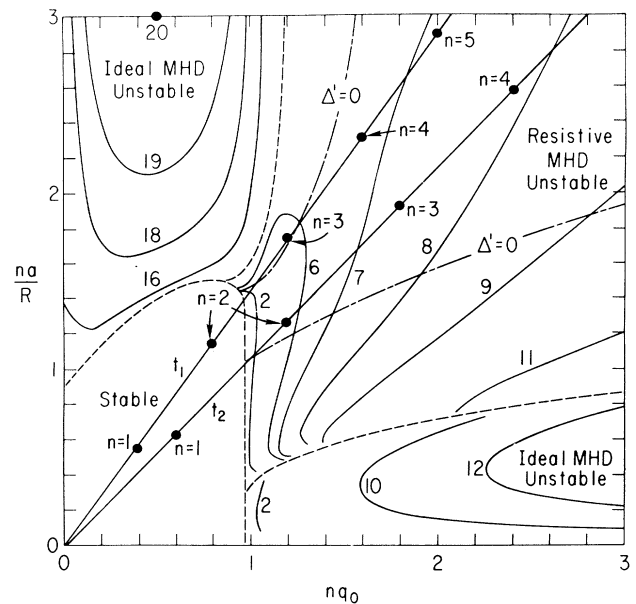


FIG. 4. Growth-rate contours of $m = 1$ perturbations. Rates are proportional to the integer labels. Stable, ideal-MHD unstable, and resistive-MHD unstable regions are distinguished by dashed curves. An equilibrium is represented by a straight line starting at the origin. Typical experimental equilibria during the period of strong mode activity are indicated at times t_1 and t_2 with $t_2 > t_1$.

$\frac{1}{3}$, and $\frac{1}{2}$ midway through the formation phase [Fig. 3(c)]. The modes follow a time sequence of $n = 5, 4, 3, 2, m = 1$ during the precise time interval that q_0 is rising through values equal to m/n . Once $q_0 > m/n$, the m/n rational surface is inside the plasma, allowing for the modes to cause a redistribution of fluxes through resistive effects. In both tokamaks and RFP's the q profile decreases during startup, while it increases in the S-1 device.

After formation, $q(\Psi)$ is a monotonically increasing function of Ψ from the separatrix ($R \approx \pm 80$ cm) to $q_0 \approx 0.7$ at the magnetic axis ($R \approx \pm 60$ cm). This general profile is maintained for the remainder of the discharge which is short compared to a resistive diffusion (hence, transport) time since a shift terminates the discharge. A classical spheromak with the same degree of oblateness as the experimental configuration is predicted to have a q_0 of 0.65, with q decreasing to 0.47 at the separatrix, in agreement with the experiment.

The experimentally observed modes and their temporal sequence is consistent with resistive-stability analysis.^{11,12} Figure 4 shows the linear-growth-rate contours¹¹ for $m = 1$ perturbations in the continuous space formed by nq_0 and na/R , where a and R are minor and major spheromak radii. An equilibrium profile is represented by a straight line emanating from

the origin. During formation, a/R increases in time, and the two straight lines with time labels t_1 and t_2 ($t_2 > t_1$) represent two experimental equilibria when the $n=3$ and $n=2$ modes are observed, respectively. Parameters q_0 , R , and a are obtained from the plots of Ψ and poloidal current RB_ϕ . The experimental trajectories of the $n=3$ and $n=2$ modes in Fig. 4 depend on the time evolutions of q_0R/a and either a/R or q_0 . The $n=2$ trajectory never enters the ideal-MHD unstable region but moves from the stable region into the resistive-MHD unstable region. Error bars on a/R admit the possibility for the $n=3$ trajectory to pass through the lower-right corner of the ideal-MHD unstable region during formation. For t_1 , modes with $n=3$ and higher are resistive-MHD unstable, while the $n=2$ mode is stable. At this time, the modes are more unstable the higher n is. It is suggested¹² that the $n=3$ mode is predominant at this time t_1 because the higher- n modes ($n \geq 4$) nonlinearly saturate at low amplitudes. At the later time t_2 , the $n=2$ mode also becomes resistive-MHD unstable. Since the $n=2$ mode is expected¹² to saturate at a relatively large amplitude compared to higher- n modes, and since the $q = \frac{1}{3}$ surface for the $n=3$ mode moves toward the edge of the plasma, one might expect the $n=2$ mode to become strong at this later time t_2 . These results are not sensitive to the plasma β (α in Ref. 11) although $\alpha=0.5$ corresponds more closely¹⁶ with the experimental β than does $\alpha=0.01$. The Hall term¹¹ is not expected to stabilize these modes since the experimental values of $\Lambda = (\omega_{ci}t_A)^{-1}$, where ω_{ci} is the ion cyclotron frequency and t_A is the Alfvén time, are below the critical value for stabilization; in addition, the above modes are near the $\Delta' = 0$ lines where Hall stabilization is not effective. It is of additional interest that the experimental equilibria are never far from the least-unstable configuration with $q_0R/a \sim 0.67$.

In summary, low- n -number resistive-MHD modes may play an important role in relaxation of the S-1 Spheromak plasma toward the Taylor state during formation, wherein there can be a large transfer of magnetic flux. The temporal evolution of modes through the $n=5, 4, 3, 2$, $m=1$ sequence parallels the rise of the experimentally measured q_0 through m/n rational

fractions. Experimental observations and comparison with theory suggest that the modes observed in the S-1 device can provide a means for relaxation since they are resonant modes and are resistive-MHD unstable.

This work was supported by the U. S. Department of Energy under Contract No. DE-AC02-76-CH0-3073.

¹M. N. Bussac *et al.*, in *Proceedings of the Seventh International Conference on Plasma Physics and Controlled Nuclear Fusion Research, Innsbruck, Austria, 1978* (International Atomic Energy Agency, Vienna, Austria, 1979), Vol. 3, p. 249.

²D. R. Wells and J. Norwood, Jr., *J. Plasma Phys.* **3**, 21 (1969).

³G. Goldenbaum *et al.*, *Phys. Rev. Lett.* **44**, 393 (1980); M. Yamada *et al.*, *Phys. Rev. Lett.* **46**, 188 (1981); J. Jarboe *et al.*, *Phys. Rev. Lett.* **45**, 1264 (1980).

⁴J. B. Taylor, *Phys. Rev. Lett.* **33**, 1139–1141 (1974).

⁵A. Janos, in *Proceedings of the Sixth U. S. Symposium on Compact Toroid Research and the Fifth U. S.–Japan Joint Symposium on Compact Toroid Research, Princeton, New Jersey, 1984* (Princeton Univ. Press, Princeton, N. J., 1984), pp. 97–102, and *Phys. Fluids* (to be published).

⁶M. Yamada *et al.*, in *Tenth International Conference on Plasma Physics and Controlled Nuclear Fusion Research, London, England, 1984* (International Atomic Energy Agency, Vienna, Austria, 1985), Vol. 2, p. 535.

⁷L. Lindberg and C. Jacobsen, *Astrophys. J.* **133**, 1043 (1961).

⁸T. R. Jarboe *et al.*, *Phys. Rev. Lett.* **51**, 39 (1983).

⁹A. C. Janos and M. Yamada, Princeton Plasma Physics Laboratory Report No. PPPL-2095, 1984, *Fusion Technol.* (to be published).

¹⁰S. C. Jardin and W. Park, *Phys. Fluids* **24**, 679 (1981).

¹¹J. DeLucia, S. C. Jardin, and A. H. Glasser, *Phys. Fluids* **27**, 1470 (1984).

¹²J. DeLucia and S. C. Jardin, *Phys. Fluids* **27**, 1773 (1984).

¹³S. V. Mirnov and I. B. Semenov, *Zh. Eksp. Teor. Fiz.* **60**, 2105 (1971) [*Sov. Phys. JETP* **33**, 1134 (1971)].

¹⁴L. A. Artsimovich, *Nucl. Fusion* **12**, 215 (1972).

¹⁵E. J. Caramana, R. A. Nebel, and D. D. Schnack, *Phys. Fluids* **26**, 1305 (1983).

¹⁶S. C. Jardin, *Nucl. Fusion* **22**, 629 (1982).